Proceedings of the Twenty-seventh (2017) International Ocean and Polar Engineering Conference **www.isope.org**
San Francisco, CA, USA, June 25-30, 2017
Copyright © 2017 by the International Society of Offshore and Polar Engineers (ISOPE)
ISBN 978-1-880653-97-5; ISSN 1098-6189

Coupled Aero-hydrodynamic Analysis on a Floating Offshore Wind Turbine under Extreme Sea Conditions

Yang Huang[1], *Decheng Wan*[1*], *Changhong Hu*[2]
[1] Collaborative Innovation Center for Advanced Ship and Deep-Sea Exploration, State Key Laboratory of Ocean Engineering, School of Naval Architecture, Ocean and Civil Engineering, Shanghai Jiao Tong University, Shanghai, China
[2] Research Institute for Applied Mechanics, Kyushu University, Fukuoka, Japan
[*]Corresponding author

ABSTRACT

To develop renewable energy, the offshore wind energy technology has become an attractive research field. Considering the coupling effect of the platform motions and aerodynamic loads, how to accurately simulate the aero-hydrodynamics of floating offshore wind turbine is important. In this paper, an unsteady actuator line model (UALM) coupled with a two-phase CFD solver called naoe-FOAM-SJTU is applied to solve the three-dimensional Navier-Stokes equations to focus on the coupled dynamic responses of an aerodynamics-hydrodynamics-mooring system for a floating offshore wind turbine named OC3-HywindSpar under extreme sea conditions. Response characteristics including the thrust and the rotor power of the wind turbine, the motions of the platform and the mooring loads under different extreme sea states are carefully compared to study the influence of the wind speed and the wave height on the floating offshore wind turbine. Furthermore, several conclusions are drawn based on the comparison results.

KEY WORDS: floating offshore wind turbine; unsteady actuator line model; extreme sea conditions; aero-hydrodynamics; couple effects.

INTRODUCTION

The increasing demand for energy and the environmental issues make the exploitation and research of new energy sources more necessary (Morató, Sriramula, Krishnan, and Nichols, 2017). As a clean renewable energy, Wind power with huge reserve is promising. The development of offshore wind power is quickly in recent years, for offshore wind is steadier and stronger than overland wind (Petersen et al., 2014). And the offshore wind energy technology has become an attractive research field in the world. Due to the complexity and particularity of ocean environment, the loads exposed on offshore wind turbines, especially on floating offshore wind turbines, are more complex than onshore wind turbines. And considering the coupling effect of the platform motions and aerodynamic loads, integrated analysis considering stochastic and wind actions for floating offshore wind turbine is challenging. So it is important to accurately simulate the aero-hydrodynamics of floating offshore wind turbine under extreme sea conditions.

It is necessary to research the coupling performance of the floating offshore wind turbine under extreme sea conditions, and some studies focusing on different aspects have been performed. Nielsen, Hanson, and Skaare (2006) combined two independent computer programs SIMO/RIFLEX and HAWC2 to a coupled simulation tool for the simulation of the dynamic response of floating wind turbines exposed to forces form wind, wave and current, and it was tested and verified to be accurate in the simulation of the performance of the whole system. M Karimirad, and Moan (2012) analyzed coupled wave and wind-induced motions of spar-type 5-MW wind turbines under operational and extreme sea states. Advanced blade element momentum theory was used to study the aerodynamics. It was found that the wind turbulence had little influence on the dynamic motion and structural responses, while it had a significant impact on power production. And the mean value of the dynamic responses of the platform was mainly induced by the wind. Muliawan, Karimirad, Gao, and Moan (2013) considered a combined concept involving a spar-type floating wind turbine and an axis-symmetric two-body wave energy converter denoted as STC, and they studied wave-wind induced response of the STC system under ultimate limit states. Coupled analysis was performed using the SIMO/TDHMILL in the time domain to investigate the force characteristics under extreme conditions. It should be noted that the wind turbine was parked under extreme conditions. It was found that the extreme responses were considered to be primarily governed by wave-induced response. And the extreme responses on the mooring line and on the bending moment at the spar-tower interface increased owing to the addition of a Torus on the floating wind turbine. M Karimirad, Gao, and Moan (2009) investigated the coupled wave and wind induced dynamic motions of the catenary moored spar floating wind turbine in harsh conditions. The DeepC code was used to calculate the displacement-force of mooring lines, and dynamic motion of the system due to wave in harsh condition was considered in HAWC2. It was found that the coupled dynamic response in harsh conditions was dominated by wind induced response. And constant wind excited the pitch natural frequency, while turbulent wind excited both surge natural frequency and pitch natural frequency. In addition, increasing the hydrodynamic damping could reduce the pitch resonance response. Ma, Hu, and Xiao (2015) discussed the effects of loads induced by wind and wave on a spar-type

floating wind turbine, and the response characteristics of motions and mooring loads of the system under operational and extreme sea states were evaluated. The calculations were made by the numerical simulation code FAST in time domain and FFT method was used in the frequency analysis. It was found that the wind-induced loads mainly influenced the low-frequency excitation but had little effect on the wave-frequency responses. It is fair to say that the research on integrated dynamic response for floating wind turbine in extreme sea conditions is limited and further research is required (Madjid Karimirad and Moan, 2010).

In this study, an unsteady actuator line model (Li, Cheng, Wan, and Xiao, 2015) coupled with a two-phase CFD solver is applied to solve the three-dimensional Navier-Stokes equations to focus on the coupled dynamic response of an aerodynamics-hydrodynamics-mooring system for a floating offshore wind turbine named OC3-hywindSpar under extreme sea conditions. The UALM is embed into the CFD solver called naoe-FOAM-SJTU to obtain the fully coupled dynamic effects with extreme load excitation. With the simulation results, aerodynamic performance parameters including the thrust and the rotor power of the floating wind turbine, detailed motion information about spar-type platform and the mooring loads can be acquired. Then, response characteristics including the thrust and the rotor power of the wind turbine, motions of the platform and the mooring loads under different extreme sea states are carefully compared. Several conclusions are drawn from the comparison results.

NUMERICAL METHOD

Unsteady Actuator Line Model

The actuator line model (ALM) which ignores the boundary layer of the blade and do not need complicated dynamic mesh is a simplified method to study the performance of the wind turbine, which can greatly decrease computation time and the total number of grids. The blade of wind turbine is divided into a series of discrete actuator units in this model (Sorensen and Shen, 2002). When the actuator line model is applied in the simulation of floating offshore wind turbines, the velocity vector (U_{motion}) caused by the motion of the platform is added into the velocity triangle (as Fig.1 shows). And there is a strong interaction between the blade and the wake. So the actuator line model need to be modified to solve the unsteady problem caused by the moving platform. And an unsteady actuator line model considering the effect of added velocity caused by the motion of the platform is used in this paper.

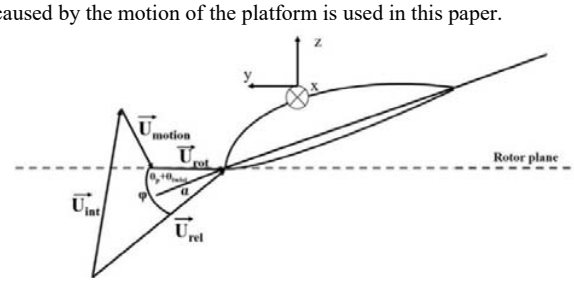

Fig.1 Velocity vector of blade's airfoil

As Fig.1 shows, the integral velocity vector relationship is described as:

$$\vec{U}_{rel} = \vec{U}_{int} + \vec{U}_{rot} + \vec{U}_{motion} \tag{1}$$

The relative wind velocity at blade section is:

$$|U_{rel}| = \sqrt{(U_{int} - U_{motion})^2 + (\Omega r - U_{rot})^2} \tag{2}$$

The inflow angle can be calculated by Eq. 3:

$$\emptyset = \tan^{-1}\left(\frac{|U_{int}| - |U_{motion}|}{|\Omega r| - |U_{rot}|}\right) \tag{3}$$

Then the attack angel of each actuator unit element can be got by Eq. 4:

$$\alpha = \emptyset - \theta_{twist} - \gamma \tag{4}$$

Where θ_{twist} and γ are local twist angle and local pitch angle of the blade respectively.

At each time step simulation, the attack angle will be updated as above described fashion, which is the difference between UALM and ALM. The volume force of each actuator unit can be acquired by the following equation:

$$f = (L, D) = \frac{\rho |U_{rel}|^2 c N_b}{2 r dr d\theta dz}(C_L e_L + C_D e_D) \tag{5}$$

Where c is the chord of the airfoil; N_b is the total number of actuator units; r is the radius at specific actuator unit; C_L and C_D stand for the lift and drag coefficient respectively.

The volume force calculated from Eq. 5 need to be smoothed by Gaussian fairing function to avoid numerical oscillation when it acts on the flow field. And the Gaussian fairing function is defined as:

$$f_\varepsilon = f \otimes \eta_\varepsilon \tag{6}$$

$$\eta_\varepsilon(d) = \frac{1}{\varepsilon^3 \pi^{3/2}} exp\left[-\left(\frac{d_i}{\varepsilon}\right)^2\right] \tag{7}$$

So the smoothing volume force can be written as:

$$f_\varepsilon(x, y, z, t) = \sum_{j=1}^{N} f_i(x_i, y_i, z_i, t) \frac{1}{\varepsilon^3 \pi^{3/2}} exp\left[-\left(\frac{d_i}{\varepsilon}\right)^2\right] \tag{8}$$

Then, f_ε is added into the 3-D N-S equation as an source term to solve the unsteady flow field of the wind turbine.

Governing Equations

A two-phase CFD solver named naoe-FOAM-SJTU developed by Professor Wan Decheng and his CFD team based on the open source tool packages OpenFOAM is used in this paper. A VOF method with bounded compression technique is applied in the solver to solve two phase flow problem with free surface. The UALM is embed into naoe-FOAM-SJTU to obtain the coupled dynamic effects of floating offshore wind turbine under extreme sea conditions. The governing equations can be written as:

$$\nabla \cdot U = 0 \tag{9}$$

$$\frac{\partial \rho U}{\partial t} + \nabla \cdot \left(\rho\left(U - U_g\right)\right) U = -\nabla p_d - g \cdot \mathrm{x} \nabla \rho + \nabla \cdot \left(\mu_{eff} \nabla U\right) + (\nabla U) \cdot \nabla \mu_{eff} + f_\sigma + f_s + f_\varepsilon \tag{10}$$

where U is velocity of field; U_g is the velocity of mesh points; $p_d = p - \rho g \cdot x$ is the dynamic pressure, subtracting hydrostatic component from total pressure; g is the gravity of acceleration vector; ρ is the mixture density with two phases; $\mu_{eff} = \rho(\upsilon + \upsilon_t)$ is effective dynamic viscosity, in which υ and υ_t are kinematic viscosity and eddy viscosity respectively; f_σ is the surface tension term in two phases model and takes effect only on the liquid free surface; f_s is the source term for sponge layer, which is set to avoid the wave reflection at the end of the tank and takes effect only in sponge layer; f_ε is the volume force calculated from UALM, representing the effect of turbine blades on the flow field.

Six Degree of Freedom (6 DoF) Motions

The 6 DoF motion solver, part of the naoe-FOAM-SJTU, is able to predict the motion of the platform, and two coordinate systems are used to solve 6DoF equation, as shown in Fig.2. They are earth-fixed coordinate system and platform-fixed coordinate system respectively. At

each time step simulation, the motion equation is solved in platform-fixed coordinate system and the force is calculated in earth-fixed coordinate equation. The added velocity vector caused by the motion of the platform in velocity triangle is updated by following equation:

$$U_{motion,i} = [J](U_c + \omega_c \cdot (x_i - x_c)) \quad (11)$$

Where $[J]$ is the transformation matrix defined from platform-fixed coordinate to earth-fixed coordinate; U_c and ω_c are the translation velocity and the angular velocity of the rotating center, respectively; x_c is the position coordinate of the rotating center.

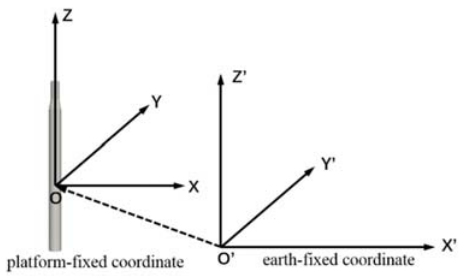

Fig.2 Two coordinate systems

NUMERICAL SIMULATION

Numerical Model

NREL offshore 5-MW baseline wind turbine developed by the U.S. Department of Energy's National Renewable Energy Laboratory is used in this paper, and its blade airfoils consist of cylinder, DU and NACA64. The main parameters of 5-MW wind turbine are given in Table 1 (J Jonkman and Musial, 2010).

Table 1 General specifications of NERL 5-MW turbine

Rating	5 MW
Rotor Orientation, Configuration	Upwind, 3 Blades
Control	Variable Speed, Collective Pitch
Drivetrain	High Speed, Multiple-Stage Gearbox
Rotor, Hub Diameter	126 m, 3 m
Hub Height	90 m
Cut-in, Rated, Cut-out Wind Speed	3 m/s, 11.4 m/s, 25 m/s
Cut-in, Rated Rotor Speed	6.9 rpm, 12.1 rpm
Rated Tip Speed	80 m/s
Overhang, Shaft Tilt, Precone Angle	5 m, 5° ,2.5°
Rotor Mass	110,000 kg
Nacelle Mass	240,000 kg
Tower Mass	347,460 kg
Coordinate Location of Overall CM (center of mass)	(-0.2 m, 0.0 m, 64.0 m)

The spar platform used in this paper is Hwindspar platform applied in OC3 project. And detailed information is listed in Table 2 (Jm Jonkman, Butterfield, Musial, and Scott, 2009).

Table 2 Main characteristics of OC3-Hwindspar platform

Depth to Platform Base Below SWL (Total Draft)	120 m
Elevation to Platform Top (Tower Base) Above SWL	10 m
Depth to Top of Taper Below SWL	4 m
Depth to Bottom of Taper Below SWL	12 m
Platform Diameter Above Taper	6.5 m
Platform Diameter Below Taper	9.4 m
Platform Mass, Including Ballast	7,466,330 kg
CML Location Below SWL Along Platform Center Line	89.9155 m
Platform Roll Inertia about CM	4,229,230,000 kg•m^2
Platform Pitch Inertia about CM	4,229,230,000 kg•m^2
Platform Yaw Inertia about Platform Centerline	164,230,000 kg•m^2

The mooring system which consists of three mooring lines is symmetrically distributed around the spar platform. Main characteristics of the mooring system are listed in Table 3. The schematic layout of the system is shown in Fig.3 (J Jonkman and Musial, 2010). And the arrangement of mooring lines is shown in Fig.4. The wind and the wave are assumed to point along the same X direction.

Table 3 Parameters of mooring system for OC3-HywindSpar platform

Number of Mooring Lines	3
Angle Between Adjacent Lines	120°
Depth to Anchors Below SWL (water depth)	320 m
Depth to Fairleads Below SWL	70.0 m
Radius to Anchors Form Platform Centerline	853.87 m
Radius to Fairleads Form Platform Centerline	5.2 m
Unstretched Mooring line length	902.2 m
Mooring Line Diameter	0.09 m
Equivalent Mooring Line Mass Density	77.7066 kg/m
Equivalent Mooring Line Mass Weight in Water	689.094 N/m
Equivalent Mooring Line Extensional Stiffness	384,243,000 N
Additional Yaw Spring Stiffness	98,340,000 Nm/rad

Fig.3 Schematic layout of the system

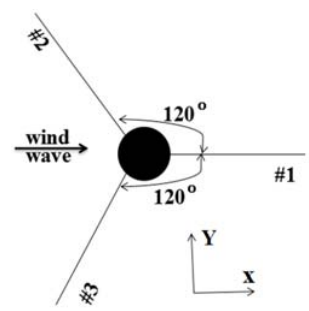

Fig.4 Mooring system

Simulation Conditions

In this paper, simulation conditions refer to Jonkman and Musial's work (2010). Linear, regular wave based on Airy theory is chosen to simulate incident wave. Wave period is 10s, and wave length is about 156m. Considering the characteristics of height-dependent wind speed, the influence of wind shear is taken into account. Exponential model is used to describe wind shear, and it can be described as:

$$u_Z = u_0 \times \left(\frac{z}{90}\right)^{0.143} \quad (12)$$

Where u_Z is the wind velocity at the height of z, u_0 is the wind velocity at the height of hub center.
Compared to Jonkman and Musial's study (2010), the effect of tower and nacelle on flow field is ignored in this paper. However, the mass and the inertial moment of the whole system including tower, nacelle, blades, platform and ballast are taken into account. In order to study the performance of the floating offshore wind turbine system under extreme sea conditions, three different extreme sea conditions are considered, and detailed simulation conditions are listed in Table 4.

Table 4 Load cases and corresponding sea states

Sea conditions	Case number	Wind velocity (u)	Significant wave height (H_s)	Peak period (T_{wave})
Extreme condition	1	5 m/s	6 m	10 s
	2	11.4 m/s	6 m	10 s
	3	11.4 m/s	10 m	10 s

Setup of Computation Domain and Boundary Condition

All numerical examples in this paper adopt the same computation domain and boundary conditions. The length and width of computation domain are 3 λ and 2 λ (λ is wave length), respectively. Considering the expansion effect of turbine wake, the height of air phase is 2 λ. The depth of water phase is set to be 70% of the real water depth (d=320m). The floating wind turbine system is placed at the middle of the computation domain, 1 λ form the inlet boundary. And the length of sponge layer before outlet boundary is 100m. The computational domain is shown in Fig.5.

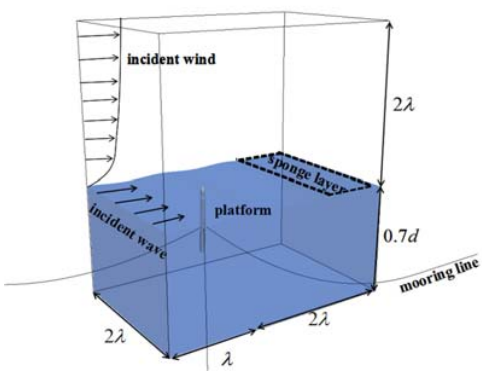

Fig.5 Setup of computational domain

To capture the wake flow of wind turbine, the refined girds are utilized in the region behind the wind turbine. And the grids near the water surface are refined to capture the free surface. Computing mesh is shown in Fig.6.

The setup of boundary conditions in numerical examples is shown below:
(1)Inlet boundary: velocity condition is wave inlet condition, and pressure condition is Neumann boundary condition that the normal gradient of pressure is equal to zero;
(2)Outlet boundary: velocity condition is inletoutlet condition defined in OpenFOAM, and pressure condition is Dirichlet boundary condition that the pressure is constant;
(3)Top boundary: both velocity condition and pressure condition are Dirichlet boundary conditions;
(4)Bottom boundary: both velocity condition and pressure condition are slip conditions;
(5)Left boundary and right boundary: boundary conditions are defined as symmetry plane that directional derivative perpendicular to the boundary is equal to zero;
(6)Body surface: the moving wall boundary condition is adopted.

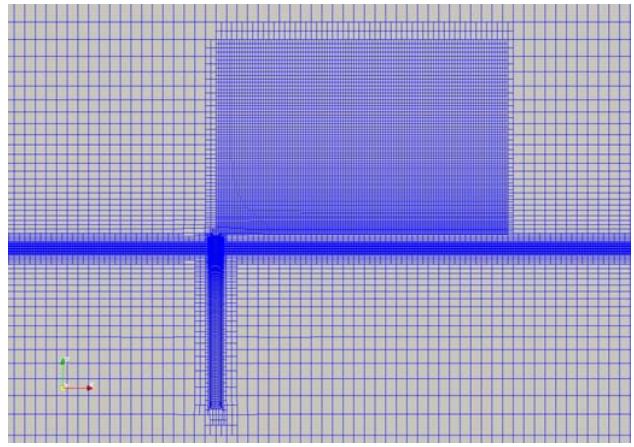
Fig.6 Computing mesh

SIMULATION RESULTS AND ANALYSIS

Aerodynamic Loads of the Wind Turbine

Numerical simulations are conducted in this paper to study the performance of the floating offshore wind turbine under extreme sea conditions. Aerodynamic loads of the wind turbine, such as the thrust and the rotor power are concerned focus.

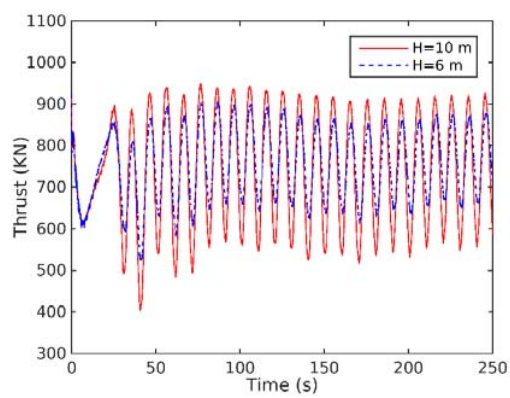

Fig.7 Comparison results of the thrust under extreme sea conditions with H_s = 6 m and H_s = 10 m. T_{wave} = 10s, u = 5 m/s.

Fig.7 shows a time series of the thrust under two different extreme sea conditions that the wave conditions are different (H_s = 6 m and H_s = 10m) and the wind conditions are the same (u=5 m/s). It can be seen that the value of the thrust is not a constant and presents periodic change over time. In addition, the change period is equal to the wave period (T_{wave} = 10 s). It suggests that the main cause for this periodic change of the thrust is the pitch motion of the platform induced by wind-wave loads, for the period of pitch motion also equals to the wave period. It can also be found that the mean value of the thrust under different wave heights are almost the same, which indicates that the wave height has a little effect on the

mean value of the thrust under extreme sea conditions. Furthermore, the variation range of the thrust under the extreme sea condition with H_s = 10 m is obviously larger than it under the extreme sea condition with H_s = 6 m. This suggests the amplitude of the variation of the thrust mainly depends on the wave height when the wind conditions are the same, which is related to the fact that pitch motion of the platform is main dominated by the wave loads.

Fig.8 shows the comparative results of the thrust under two different extreme sea conditions that the wind conditions are different (u = 5 m/s and u = 11.4 m/s) and the wave conditions are the same (H_S = 6 m). It can be seen that the mean value of the thrust significantly increases with the wind velocity, which is an obvious fact that the thrust is mainly dominated by the wind loads. And the variation range of the thrust also increases with the wind velocity, which indicates not only the wave height but also the wind velocity has a noticeable effect on the thrust. Furthermore, it can also be seen that the thrust becomes more unsteady with the increase of the wind velocity.

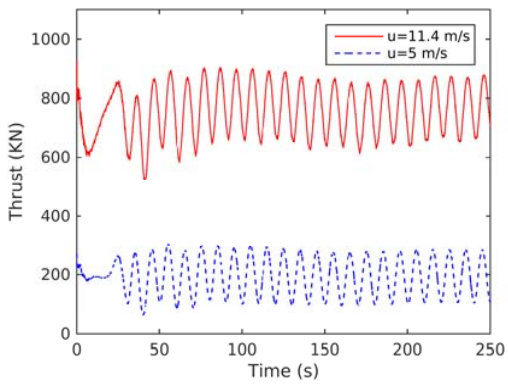

Fig.8 Comparison results of the thrust under extreme sea conditions with u = 5 m/s and u = 11.4 m/s. H_s = 6 m, T_{wave} = 10s.

As shown in Figs.9~10, the rotor power of the wind turbine under different wave conditions (H_s = 6 m and H_s = 10m) and different wind conditions (u = 5 m/s and u = 11.4 m/s) are carefully compared. And compared to Figs. 7~8, it can be found that the effect of the wave height and the wind velocity on the rotor power is similar to the effect on the thrust.

Fig.9 shows a time series of the rotor power under two different extreme sea conditions that the wave conditions are different (H_s = 6 m and H_s = 10m) and the wind conditions are the same (u=5 m/s). It can be found that the value of the rotor power shows obvious cyclic change and the change period is equal to the wave period. The mean value of the rotor power under different wave heights are almost the same, which indicates that the wave height has a little influence on the mean value of the rotor power. And the change range of the rotor power increases with the wave height when the wind loads are the same. This indicates that the wave height has a significant impact on the amplitude of the variation of the rotor power.

Fig.10 shows the comparative results of the rotor power under two different extreme sea conditions that the wind conditions are different (u = 5 m/s and u = 11.4 m/s) and the wave conditions are the same (H_S = 6 m). It can be seen that the mean value of the rotor power increases with the wind velocity, which indicates that mean value of the rotor power primary depends on the wind velocity. And the variation range of the rotor power significantly increases with the wind velocity, which indicates the wind velocity has a significant effect on the amplitude of the variation range of the rotor power.

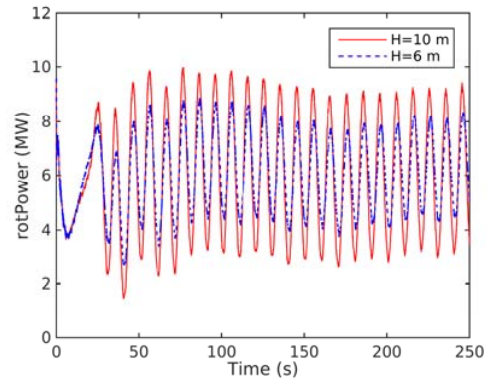

Fig.9 Comparison results of the rotor power under extreme sea conditions with H_s = 6 m and H_s = 10 m. T_{wave} = 10s, u = 5 m/s.

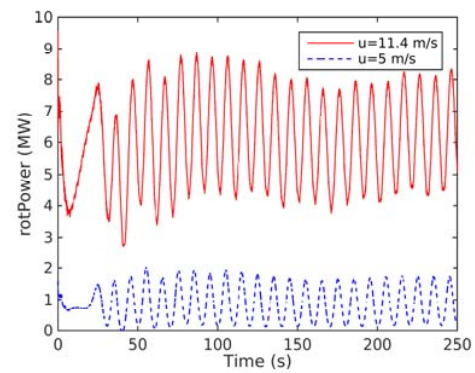

Fig.10 Comparison results of the rotor power under extreme sea conditions with u = 5 m/s and u = 11.4 m/s. H_s = 6 m, T_{wave} = 10s.

As analyzed in the above, the aerodynamic loads of the floating offshore wind turbine change in a cyclical manner caused by the motion of the platform induced by wind-wave loads. The amplitude of the variation increases with the wave height and the wind velocity. And the wind velocity has a significant effect on the mean value of the thrust and the rotor power. Besides, the values of the thrust and the rotor power vary in a wide range under extreme sea conditions, which means the whole system will suffer more serious fatigue loading. The rapid development of the thrust and rotor power demand a higher requirement on the security and steadily of the system, which should be considered in the design stage of the floating off shore wind turbine.

Wake Vortex

The wake vortex structure of the wind turbine under the extreme sea state is analyzed here. Fig.11 shows the wake vortex structure at different times of one wave period under the extreme sea condition that the wind velocity is the rated 11.4 m/s and the wave height is 10 m. Vortex structure is represented by the magnitude of the square of velocity gradient. The color of wave surface represents the wave height. It can be seen that clear spiral vortex is produced at the tip of the blades. However, the tip vortex quickly expands and fragments with time. The root vortex presents a spiral structure, and it also fragments rapidly. This indicates that the wake vortex under extreme sea conditions is highly unsteady, in part because the wake vortex interacts with the wake due to the pitch motion of the platform.

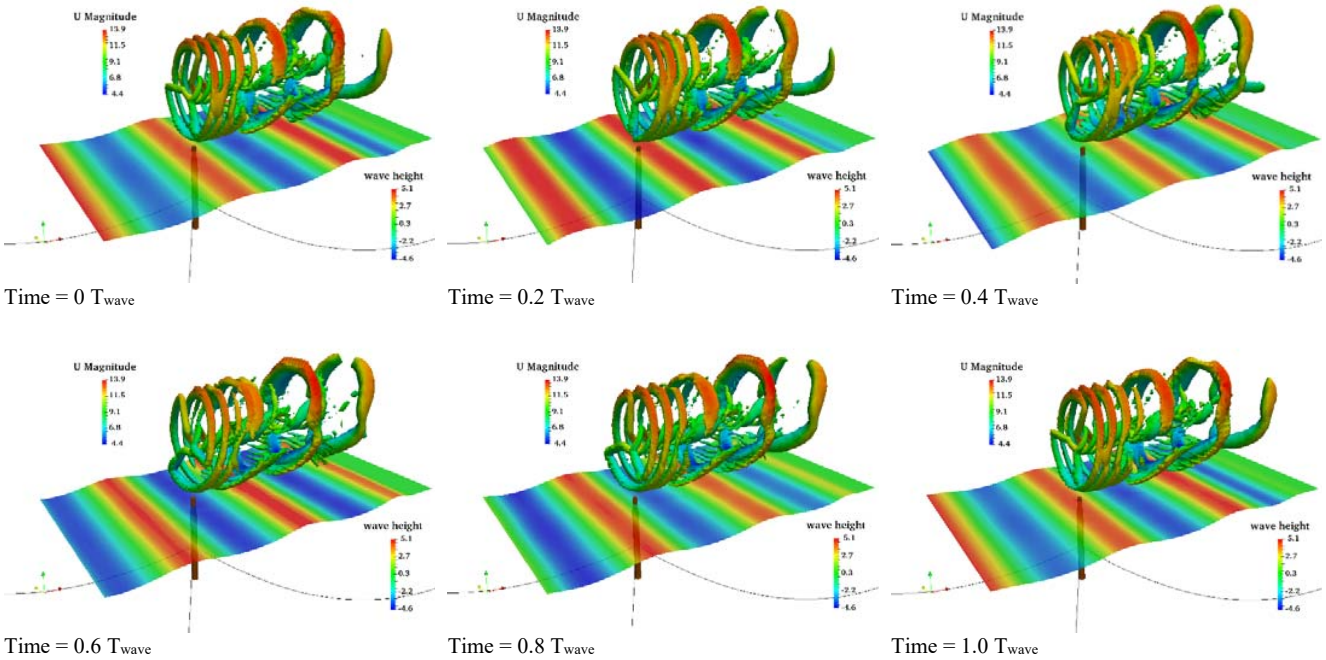

Fig.11 Trailing vortex structure at different times of one wave period under the extreme sea condition with Hs=10 m, T_{wave} =10 s, u=11.4 m/s.

Wind-wave Induced Motion of the Platform

Fig.12 shows the comparative results of the motion responses of the platform induced by wind-wind loads under extreme sea conditions that the wave conditions are different (H_s = 6 m and H_s = 10m) and the wind conditions are the same (u=5 m/s). It can be seen that the six-degree-freedom motions of the platform are periodic motions, and the motion period of different degree of freedom motions are different. Besides, the motion responses of the platform including the motion amplitude and motion trend are almost the same under the different wave heights, and there is a slight increase of amplitude for heave motion and pitch motion when the wave height is 10m. It indicates that the wave height has a little effect on the motion responses of the platform induced by wind-wave loads under extreme sea conditions, which is unusual for the responses of the platform. Considering the coupling effect of the platform and the wind turbine, the cause for this phenomenon could be that the responses of the platform are mainly induced by the aerodynamic force derived from the wind turbine system under extreme sea conditions. And further researches should be conducted to discuss the mechanisms behind this phenomenon.

Interestingly, Fig.13, which shows the comparison results of the motion responses of the platform under extreme sea conditions that the wind conditions are different (u = 5 m/s and u = 11.4 m/s) and the wave conditions are the same (Hs = 6 m), may explain the above phenomenon in part. It can be seen that there is a significant increase of motion amplitude for the six-degree-freedom motions responses of the platform when the wind velocity is 11.4 m/s. This suggest that the wind loads have a remarkable impact on the motion responses of the platform induced by wind-wave loads under extreme sea conditions.

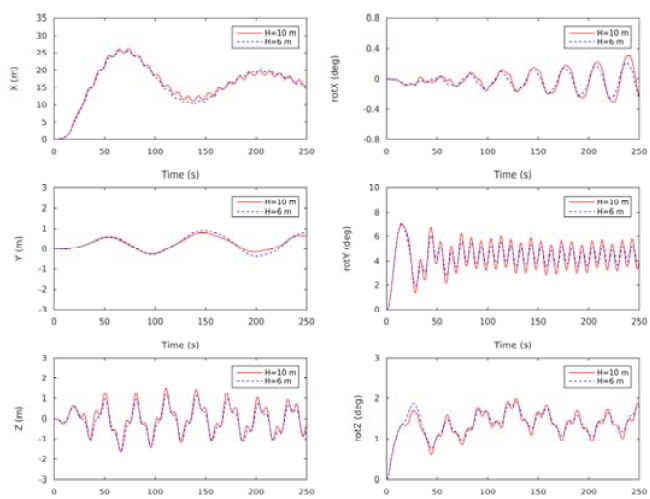

Fig.12 Comparison results of six-degree-freedom motions responses of the platform under extreme sea conditions with H_s = 6 m/s and H_s = 10 m. T_{wave} = 10s, u = 5 m/s.

Synthesizing the above analysis, the motion responses of the platform induced by wind-wave loads under extreme sea conditions is dominated mainly by the wind loads, so more attention should be paid to the wind loads in the design stage of floating offshore wind turbine.

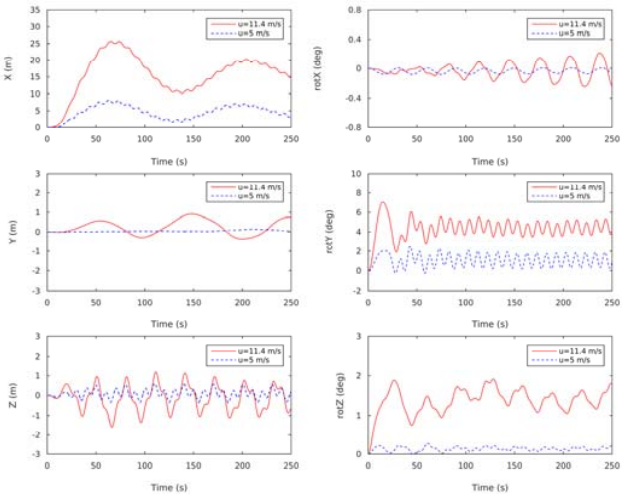

Fig.13 Comparison results of six-degree-freedom motions responses of the platform under extreme sea conditions with u = 5 m/s and u = 11.4 m/s. Hs = 6 m/s, T_{wave} = 10s.

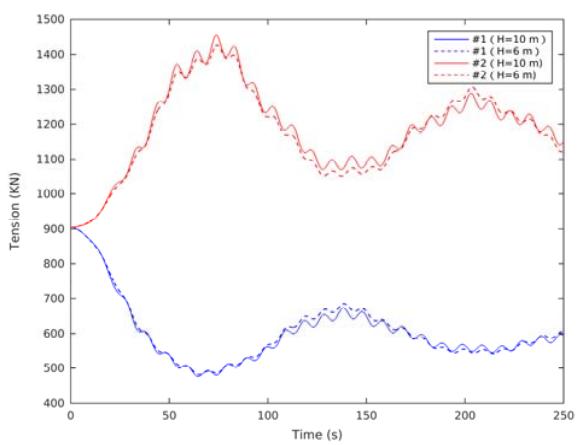

Fig.14 Comparison results of the mooing tension of mooring line 1 and 2 under extreme sea conditions with H_s=6 m and H_s=10 m. T_{wave}=10 s, u = 11.4 m/s.

Mooring Tension

Considering the facts that the mooring lines are symmetrically distributed about X axis and the directions of the wind and the wave are both set to along X axis, only the mooring tensions of line 1 and line 2 are analyzed here. As shown in Figs.14~15, the mooring tensions under the different wave heights (H_s = 6 m and H_s = 10m) and the different wind velocities (u = 5 m/s and u = 11.4 m/s) are carefully compared. And compared to Figs.12~13, it can be found that the trend of the mooring tension is similar to the surge motion of the platform, which is an obvious fact that the mooring loads is mainly dominated by the surge motion. The tensions of mooring lines are almost the same when the wind conditions are the same. However, the mooring tension significantly increases with the wind velocity. It indicates that the mooring tension is mainly dominated by wind-induced loads and the wave height has a little influence on the mooring tension. In addition, the variation tendency of mooring tension of line 1 is opposite to that of line 2, which is related to the arrangement of mooring line.

It should be noted that the variation range of the mooring tension under extreme sea conditions is great due to the large drift displacement of the platform, so there is a risk of failure for the mooring lines under extreme sea conditions.

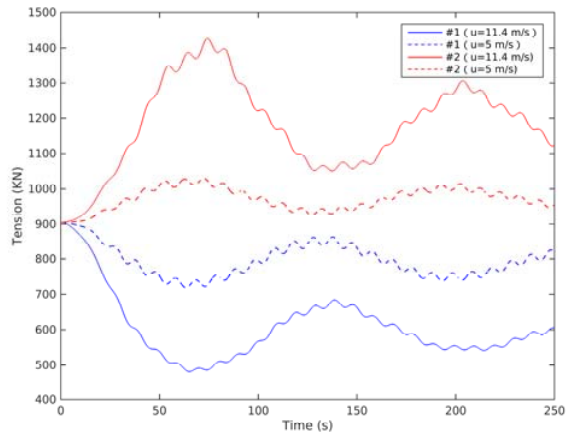

Fig.15 Comparison results of the mooing tension of mooring line 1 and 2 under extreme sea conditions with u = 5 m/s and u = 11.4 m/s. H_s=6 m, T_{wave}=10 s.

CONCLUSIONS

In this paper, an UALM coupled with a two-phase CFD solver called naoe-FOAM-SJTU is applied to solve the three-dimensional Navier-Stokes equations. And the coupled dynamic responses of a spar-type floating wind turbine induced by wind and wave loads under different extreme sea conditions are analyzed. Several conclusions can be drawn from the above analysis. First, the thrust and the rotor power of the wind turbine represent periodic change over time when the coupling effect of the hydrodynamic-aerodynamic-mooring system is considered. And the mean value of the aerodynamic loads is mainly dominated by the wind loads, whereas the fluctuation range of the aerodynamic loads is mainly depend on the wave loads. In addition, the wake vortex of the wind turbine is highly unsteady under extreme sea conditions. Second, the motion responses of the platform induced by wind-wave loads under extreme sea conditions are dominated mainly by the wind loads, and the motion responses of the platform under the different wave heights are almost the same. Third, the trend of mooring tension coincides with the surge motion of the platform, and the variation range of the mooring tension is large under extreme sea conditions. So the risk of failure for mooing lines caused by the large drift displacement of the platform under extreme sea conditions should be considered.

ACKNOWLEDGEMENTS

This work is supported by the National Natural Science Foundation of China (51379125, 51490675, 11432009, 51579145), Chang Jiang Scholars Program (T2014099), Shanghai Excellent Academic Leaders Program (17XD1402300), Shanghai Key Laboratory of Marine Engineering (K2015-11), Program for Professor of Special Appointment (Eastern Scholar) at Shanghai Institutions of Higher Learning (2013022), Innovative Special Project of Numerical Tank of Ministry of Industry and Information Technology of China(2016-23/09) and Lloyd's Register Foundation for doctoral student, to which the authors are most grateful.

REFERENCES

Jonkman, J., Butterfield, S., Musial, W., and Scott, G. (2009). Definition of a 5-MW reference wind turbine for offshore system development. *Contract*, (February), 1–75. https://doi.org/10.1002/ajmg.10175

Jonkman, J., and Musial, W. (2010). Offshore code comparison collaboration (OC3) for IEA task 23 offshore wind technology and deployment. *Contract*, *303*(December), 275–3000.

Karimirad, M., Gao, Z., and Moan, T. (2009). Dynamic motion analysis of catenary moored spar wind turbine in extreme environmental condition. *... the European Offshore Wind ...*, (May 2016).

Karimirad, M., and Moan, T. (2010). Extreme Structural Dynamic Response of a Spar Type Wind Turbine. *29th International Conference on Ocean, Offshore and Arctic Engineering: Volume 3*, (January), 303–312.

Karimirad, M., and Moan, T. (2012). Wave-and Wind-Induced Dynamic Response of a Spar-Type Offshore Wind Turbine. *Journal of Waterway, Port, Coastal, and Ocean Engineering*, *138*(1), 9–20.

Li, P., Cheng, P., Wan, D.C., and Xiao, Q. (2015). Numerical Simulations of Wake Flows of Floating Offshore Wind Turbines by Unsteady Actuator Line Model, (August), 26–28.

Ma, Y., Hu, Z. Q., and Xiao, L. F. (2015). Wind-wave induced dynamic response analysis for motions and mooring loads of a spar-type offshore floating wind turbine. *Journal of Hydrodynamics*, *26*(6), 865–874.

Morató, A., Sriramula, S., Krishnan, N., and Nichols, J. (2017). Ultimate loads and response analysis of a monopile supported offshore wind turbine using fully coupled simulation. *Renewable Energy*, *101*, 126–143.

Muliawan, M. J., Karimirad, M., Gao, Z., and Moan, T. (2013). Extreme responses of a combined spar-type floating wind turbine and floating wave energy converter (STC) system with survival modes. *Ocean Engineering*, *65*, 71–82.

Nielsen, F. G., Hanson, T. D., and Skaare, B. (2006). Integrated dynamic analysis of floating offshore wind turbines. *Proceedings of the 25th International Conference on Offshore Mechanics and Arctic Engineering*, (January 2017), 671–679.

Petersen, E. L., Hasager, C. B., Courtney, M., Natarajan, A., Larsen, T. J., Bredmose, H., … Erik-clausen, N. (2014). *Offshore Wind Farms*.

Sorensen, J. N., and Shen, W. Z. (2002). Numerical Modeling of Wind Turbine Wakes. *Journal of Fluid Engineering*, *124*(June 2002), 393–399.